JOURNAL OF Applied Polymer SCIENCE

Study on the Biocomposites with Poly(ethylene glycol) Dimethacrylate and Surfaced-Grafted Hydroxyapatite Nanoparticles

Haibo Li, Yi Fu, Rui Niu, Ziyou Zhou, Jun Nie, Dongzhi Yang

Key Laboratory of carbon fiber and functional polymers, Ministry of Education, Beijing University of Chemical Technology, Beijing 100029, China

Correspondence to: D. Yang (E-mail: yangdz@mail.buct.edu.cn)

ABSTRACT: In composites of hydroxyapatite (HA) nanoparticles with a polymer matrix, the aggregation of nanoparticles would induce structural defects. In order to improve the dispersibility of HA nanoparticles in poly(ethylene glycol) dimethacrylate (PEGDMA) matrix and enhance mechanical properties of the HA/PEGDMA composite as potential bone substitute material, surface-grafted HA nanoparticles with poly(ethylene glycol) monomethacrylate (PEGMA) were prepared, and crosslinked with PEGDMA under UV light to form a composite. The structure of HA-*g*-PEGMA was characterized by X-ray diffraction (XRD) and thermal gravimetric analysis (TGA). The dispersibility of HA-*g*-PEGMA nanoparticles in poly(PEGDMA) was evaluated by SEM. The mechanical properties of the composites were investigated by compressive test. The dispersibility of HA-*g*-PEGMA nanoparticles in poly(PEGDMA) matrix was better than the bare HA. At a 1 wt % content of loading, the strength of composites increased by 14%, and the modulus increased by 9%. © 2012 Wiley Periodicals, Inc. J. Appl. Polym. Sci. 000: 000–000, 2012

KEYWORDS: composites; nanoparticles; photopolymerization; hydroxyapatite; surface grafting; poly(ethylene glycol) dimethacrylate

Received 21 February 2011; accepted 13 March 2012; published online
DOI: 10.1002/app.37732

INTRODUCTION

Synthetic hydroxyapatite (HA) has already been widely used in clinic due to its similarity to inorganic component of human natural bone in structure and composition. It has good biocompatibility to human tissue.[1–7] For possible bone tissue engineering applications, composites of HA particles and polymer matrix such as chitosan[8,9] and collagen[10,11] were prepared. However, it was difficult for HA to uniformly disperse in the polymer matrix, and aggregation of HA was very common. Therefore, the mechanical properties of composites were greatly reduced.[12,13] The interface adhesion of HA particles and polymer matrix played a very important role among the major factors affecting the properties of the HA/polymer composites. In order to increase the interfacial strength between the two phases, various methods have been employed. For example, Chen and coworkers[14–16] used the ring-opening polymerization of L-lactide on the surface of HA and esterification of poly-L-lactide acid (PLLA) and HA. HA nanoparticles could be uniformly dispersed in the PLLA matrix and showed improved adhesion with PLLA matrix. Therefore, the HA-*g*-PLLA/PLLA composites exhibited better mechanical properties than that of simple *n*-HA/PLLA blends. Liu et al.[17–19] used isocyanate to react with hydroxyl groups on the surface of HA to prepare the poly(ethylene glycol)(PEG)/HAp and polymethyl methacrylate (PMMA)/HAp composites by diisocyanate modifying HA surface with polymer. Pramanik et al.[20] found that the phosphonic acid group of 2-carboxyethylphosphonic acid could strongly anchor on apatite surface while the active carboxyl terminal enhanced chemically bonded interactions with the hydroxyl groups of the polymer, thus improved the interfacial bonding between HA nanoparticles and poly(ethylene-*co*-vinyl alcohol) matrix.

In our previous study,[21,22] HA nanoparticles were formed in poly(ethylene glycol) dimethacrylate (PEGDMA) *in situ*. The composites had well dispersity of inorganic phase and better mechanical behavior, compared to composite of physical mixing of HA and PEGDMA. PEGDMA is one kind of unsaturated linear polyether with main chain of polyethylene glycol and end groups of methacrylate which could be photocrosslinked *in situ*. Cured PEGDMA was biocompatible and mildly cytotoxic.[23] In the bone tissue engineering field, PEG, the main chain of PEGDMA, could reduce the protein adsorption and cell adhesion on the surface of bone substitution, which would improve the bone remodeling.[24]

In this work, HA nanoparticles were surface modified by 4-methyl-*m*-phenylene diisocyanate (TDI), then grafted with poly(ethylene glycol) monomethacrylate (PEGMA). The grafted HA nanoparticles crosslinked with PEGDMA to form the composites without aggregation of nanoparticles, and the nanoparticles could uniformly distribute in PEGDMA matrix. Therefore, the improvement of mechanical property of composite was achieved.

EXPERIMENTAL SECTION

Materials

PEG (M_w = 600) was purchased from Beijing Chemical Reagents Company (Beijing, China). Poly(ethylene glycol) dimethacrylate (PEGDMA600) was donated by Sartomer Company (Guangzhou, China). Methacryloyl chloride was purchased from Shanghai Chemical Reagents Company (Shanghai, China). Photoinitiator 2959 (Darocur 2959, 2-hydroxy-1-4-(hydroxyethoxy) phenyl-2-methyl-1-propanone) was supplied from Ciba-Geigy Chemical Co. (Tom River, NJ). HA (20 nm average diameter, 100 nm average length) was purchased from Sinopharm Chemical Reagent (Shanghai, China). TDI was purchased from Kaicheng Chemical Co. (Changzhou, China). Dibutyltion dilaurate (DBTDL) as catalyst was purchased from Aladdin Reagent Co. (Shanghai, China).

Synthesis of Poly(ethylene glycol) Monomethacrylate. 2.64 g triethylamine and 0.02 mol PEG (M_w = 600) were dissolved in 500 mL of chloroform in a three-necked flack equipped with stirrer, thermometer, and dropping funnel, under cooling. 2.1 g methacryloyl chloride dissolved in 50 mL of chloroform was dropped into the mixture in the flack within 3 h. After dropping, the mixture was stirred overnight. The reacted solution was filtered and then the filtered liquid was extracted three times with 1 mol/L HCl solution, 1 mol/L $NaHCO_3$ solution, and deionized water, successively. Then, anhydrous Na_2SO_4 was added to get rid of residual water. In the end, chloroform was removed by rotary evaporation. The yellow liquid product was dried under vacuum at room temperature overnight.

Grafting of PEGMA on the Surface of Hydroxyapatite Nanoparticles. 0.01 mol PEGMA and 8 drops of DBTDL were dissolved in 50 mL of chloroform in a three-necked flack at 30°C. Solution of 1.72 g TDI in 50 mL chloroform was dropped into the mixture within 3 h under continuous stirring and nitrogen protection. Next, the mixture was removed into another dropping funnel, then dropped into HA suspension containing 2 g HA nanoparticles, 100 mL chloroform, and 0.2 mL of DBTDL at 45°C for 3 h under nitrogen protection and continuous stirring. Then the reaction mixture was cooled down to room temperature. The HA-*g*-PEGMA particles were separated by centrifugation at 5000 rpm and washed with excessive chloroform for five times to completely remove the free PEGMA and TDI. It indicated that the free PEGMA and TDI were washed away, when the characteristic peaks at 3347 cm^{-1} attributed to —OH and at 2267 cm^{-1} attributed to —NCO disappeared. Finally, the separated sediment was dried in a vacuum oven at 35°C for 24 h to remove the residual chloroform. The scheme of preparation is shown in Figure 1.

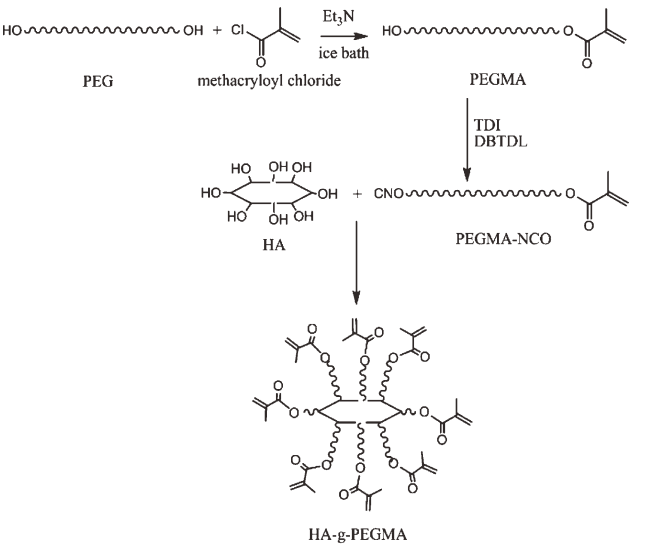

Figure 1. The preparation process of HA-*g*-PEGMA.

Preparation of PEGDMA/HA-g-PEGMA and PEGDMA/HA Composites. The PEGDMA/HA-*g*-PEGMA and PEGDMA/HA composites were prepared as follows: pre-weighed dried HA or HA-*g*-PEGMA powders were uniformly suspended in PEGDMA with intensively magnetic stirring and ultrasonic, separately. One weight percent of monomer weight of photoinitiator 2959 was added into the above solution based on monomer. Then the above solution was injected into the cylindrical molds, which are 10 mm of diameter and 10 mm of thickness for compressive test, and irradiated with UV light source (320–480 nm, EXFO lite, EFOS Corporation, Mississauga, Canada) under light intensity 30 mW/cm^2 for 10 min to form composites.

Fourier Transform Infrared Spectra Study. Fourier transform infrared (FTIR) spectrum was recorded by a Nicolet 5700 instrument (Nicolet Instrument, Thermo Company, Wisconsin-Madison, USA). Samples were prepared as KBr pellet and scanned against a blank KBr pellet background at wavenumber range 4000–650 cm^{-1} with resolution of 4.0 cm^{-1}. The polymerization process of composites was monitored by using series real time near infrared spectroscopy (RTIR, Nicolet 5700 instrument, Thermo Company, USA). RTIR technology has been widely used to measure the conversion of methacrylate monomers under irradiation. The integral area of =C—H absorption peak from 6110 to 6210 cm^{-1} is directly proportional to the amount of polymerized methacrylate. During irradiation, the decrease of the =C—H absorption peak area accurately monitored by instrument, which reflects the extent of photopolymerization.

X-ray Diffraction Study. X-ray diffraction (XRD) patterns of the HA-*g*-PEGMA nanoparticles were recorded on a X-ray diffractometer (D/Max2500VB2+/Pc, Rigaku, Japan) at a voltage of 40 kV and a current of 50 mA with Cu Kα characteristic radiation (wavelength = 0.154 nm). The scanning rate was 5°/min and the scanning scope of 2θ was from 5° to 90° at room temperature.

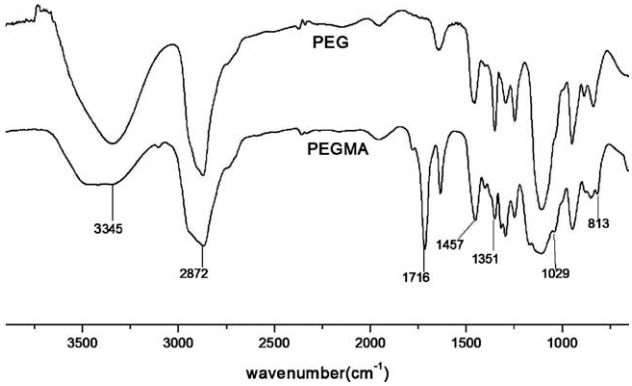

Figure 2. IR spectra of PEG and the product of PEG reacted with methacryloyl chloride.

Thermal Gravimetric Analysis. Thermal gravimetric analysis (TGA) was carried out with a NETZSCH TG 209 F1 analyzer (NETZSCH Instruments Co., Ltd., Germany) from 25°C to 580°C with heat rate of 10 °C/min under air condition.

Scanning Electron Microscopy Study. The morphology of composites was determined by scanning electron microscopy (SEM; S-450, Hitachi Ltd, Japan) at an accelerating voltage of 20 kV. To obtain morphology, specimen was immersed into liquid nitrogen, fractured, and then sputter coated with a thin layer of gold.

Mechanical Properties. The mechanical properties of composites were tested by compression mode. For samples preparation, the PEGDMA/HA-*g*-PEGMA or PEGDMA/HA solution was injected into a cylindrical mold of 10 mm of diameter and 10 mm of thickness. For 10 min under UV irradiation (30 mW/cm^2), the cured samples were obtained. The samples were tested by universal testing machine (Model 1185, Instron, USA) with a speed of 5 mm/min at room temperature. All experiments were repeated three times.

Cell Adhesion. After sterilized in 70% ethanol for 24 h and extensively washed three times with sterile 0.01 mol/L phosphate buffer solution (PBS, pH = 7.4), the disk samples of pure PEGDMA, HA/PEGDMA, and HA-*g*-PEGMA/PEGDMA for cell culture were incubated in the culture medium overnight at 37°C, and then the medium was removed. Human mesenchymal stem cells (hMSCs), which was often used in bone tissue engineering to evaluate the biocompatibility of biomaterials, were cultured in Dulbecco's Modified Eagle Medium (Gibco, Invitrogen Corporation, NY) supplemented with 10% fetal bovine serum (Sigma–Aldrich, St. Louis, MO), 100U/mL penicillin (Sigma–Aldrich, St. Louis, MO), and 100 μg/mL streptomycin (Sigma–Aldrich, St. Louis, MO). Cells were incubated at 37°C in a 5% CO_2 incubator and the medium was changed every 2 days. When the cells reached the stage of confluence, they were harvested by trypsinization followed by the addition of fresh culture medium to create a cell suspension. A cell suspension with a concentration of 1 × 10^6 cells/mL was loaded on the surface of samples, with 200 μL of suspension for each sample. The composites were put in a polystyrene 48-well culture plate and incubated at 37°C in a 5% CO_2 incubator.

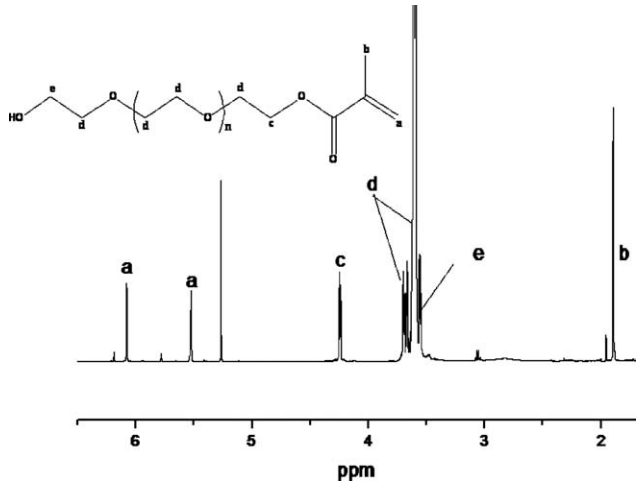

Figure 3. ^{1}H-NMR spectrum of the product of PEG reacted with methacryloyl chloride with CD_3Cl as solvent.

hMSCs suspension with a concentration of 1 × 10^6 cells/mL was seeded on the surface of samples. The samples were put in a 48-well culture plate and incubated at 37°C in a 5% CO_2 incubator. Digital images of the hMSCs were collected from an inverted phase contrast microscope after 3 days of culture.

RESULTS AND DISCUSSION

PEGMA

PEGMA was synthesized by esterification reaction of PEG and methacryloyl chloride. The FTIR transmittance spectrum of PEGMA is shown in Figure 2. The principal characteristic spectrum of PEG could be seen in the figure: 1029 cm^{-1} (O—H stretch), 1351–1457 cm^{-1} (—CH bend), 2872 cm^{-1} (C—H stretch), 3345 cm^{-1} (O—H stretch). After esterification reaction with methacryloyl chloride, characteristic peaks at 1716 cm^{-1} (C=O stretch) and 813 cm^{-1} (C=C) appeared in PEGMA spectrum, which indicated that the methacryloyl chloride have reacted with hydroxyl group of PEG.

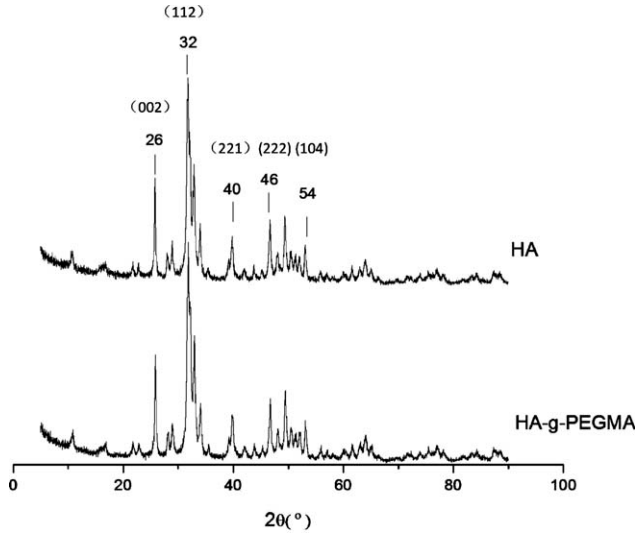

Figure 4. XRD patterns of HA and HA-*g*-PEGMA.

Applied Polymer SCIENCE

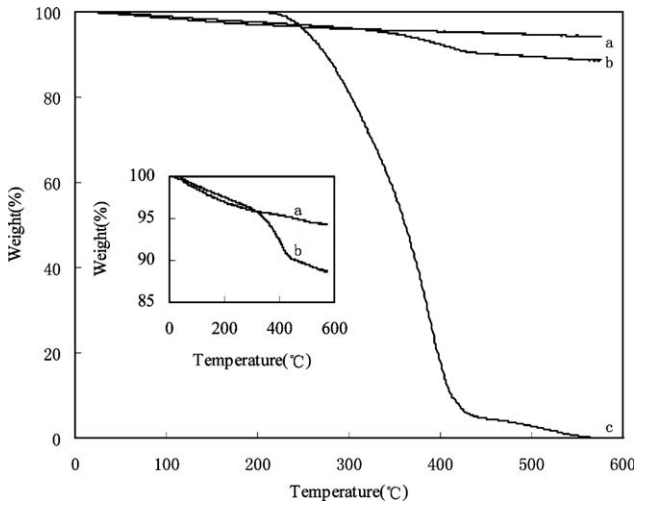

Figure 5. TGA thermograms of HA and HA-*g*-PEGMA. (a) HA, (b) HA-*g*-PEGMA, (c) PEGMA.

The ^{1}H-NMR spectra of PEGMA in CD_3Cl is shown in Figure 3. The signals from the methacryloyl group were observed at 5.75 and 6.2 ppm (protons at the double bond, H_a) as well as at 1.95ppm (methyl protons, H_b), having an ratio (H_b : H_a)of 3 : 2 as expected. The signals from methylene next to ester group were observed at 4.24 ppm (methylene protons, H_c). The signals from methylene next to hydroxy were observed at 3.55 ppm (methylene protons, H_e). According to the ^{1}H-NMR spectra, A_a : A_c : A_e = 2 : 2 : 2 in which A stand for the average area of peaks. It confirmed that the product was PEGMA.

X-ray Diffraction Study

The XRD patterns of HA and HA-*g*-PEGMA are shown in Figure 4. The HA and HA-*g*-PEGMA exhibited the same sharp peaks at 2θ regions of 26°, 32–34°, 40°, and 46–54° which are the same as the crystalline nature of hexagonal HA($P6_3/m$, JCPDs card No.9-432).[25,26] This confirmed that the grafting reaction on the surface of HA nanoparticles does not cause crystalline form change and secondary phases formed.

Thermal Gravimetric Analysis

The grafting amount of PEGMA on the HA was confirmed by TGA. TGA curves of the HA and the HA-*g*-PEGMA nanoparticles are shown in Figure 5. The bare HA displayed a weight loss at temperature from 20 to 580°C, in which the losing rate decreased above 312°C. This was attributed to the evaporation of intra water in the HA at elevated temperature. Thermogravimetric analysis of bare HA powder was consistent with literature reported trends.[27] For the HA-*g*-PEGMA, the sample lost weight very fast from 312 to 580°C in comparison to the bare HA sample, which could be attributed to the decomposition of the organic group (as well as the evaporation of water) from the HA surface. The grafted ratio on the surface of PEGMA was calculated by the following equation, W_1 and W_0 are the weight loss of HA and HA-*g*-PEGMA, respectively.

$$\text{The grafting ratio} = W_1(\%) - W_0(\%)$$

The grafted amount of PEGMA determined by TGA analysis was approximately 6 wt %.

Photopolymerization of Composite

The double bond of HA-*g*-PEGMA and PEGDMA started to copolymerize and area of double bond absorbance peak near 6140–6210 cm^{-1} decreased under UV irradiation. The polymerization of HA-*g*-PEGMA /PEGDMA led to high conversion of double bond in a few minutes, as shown in Figure 6(a). There was no obvious difference between the conversion rate of the composites containing HA or HA-*g*-PEGMA, and double bond conversion reached to 100%. As shown in Figure 6(b), the conversion rate of composites decreased with the increase of content of HA-*g*-PEGMA. HA nanoparticles could absorb the UV light, so the increase of content of nanoparticles would hinder the photopolymerization progress and decelerate the conversion rate of composites.

Morphology Analysis

The morphology of the composites with 5 wt % HA or HA-*g*-PEGMA was examined by SEM, as shown in Figure 7. A typical HA particle is denoted by arrows in the pictures. HA in composites modified on the surface dispersed well at nano-scale, while

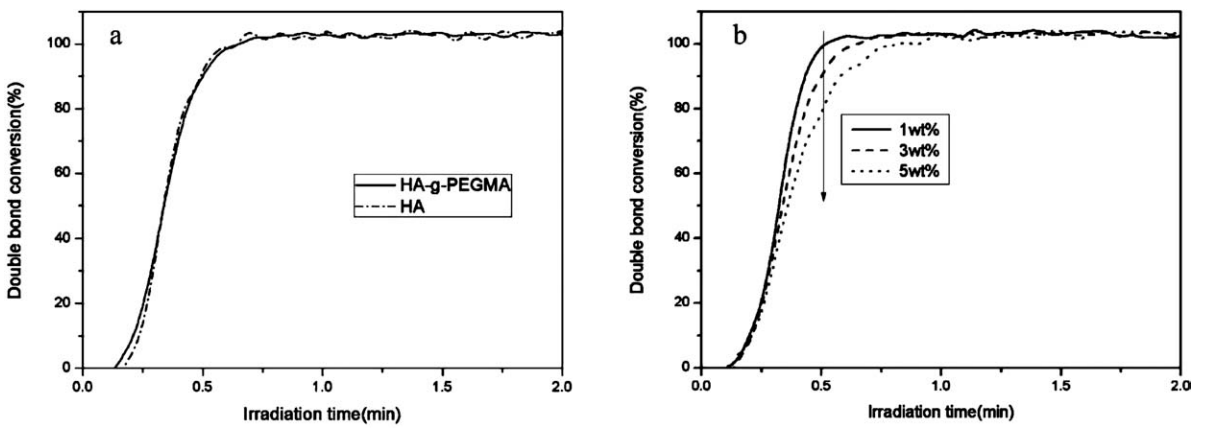

Figure 6. Double bond conversion vs. irradiation time of photopolymerization of composite: (a) HA and HA-*g*-PEGMA; (b) 1 wt %, 3 wt %, and 5 wt % of HA-*g*-PEGMA in composite.

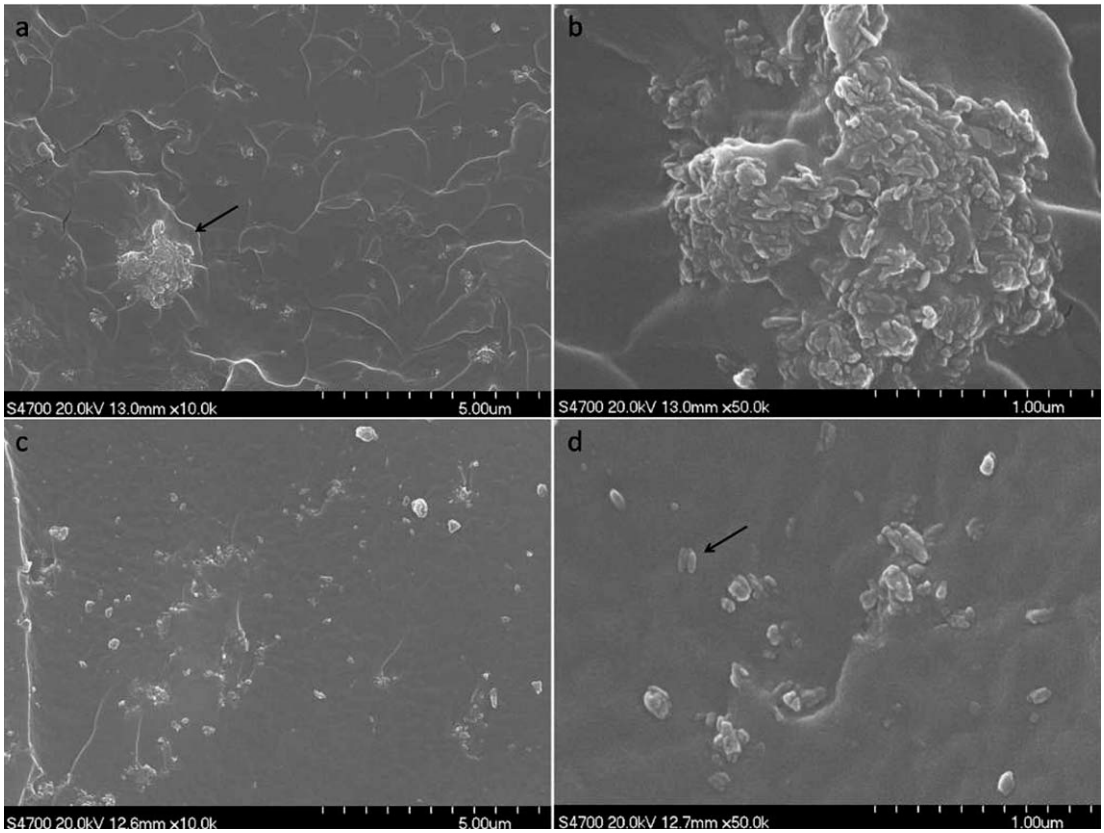

Figure 7. SEM images of composites. (a) composites with bare HA nano-particles, ×10,000; (b) composites with bare HA nano-particles, ×50,000; (c) composites with HA-*g*-PEGMA nano-particles, ×10,000; (d) composites with HA-*g*-PEGMA nano-particles ×50,000.

bare HA powders in composites made by mixing aggregated to a micron-scale extent. Comparing the morphology of both composites, it confirmed that bare HA nanoparticles in composites aggregated to a micron-scale extent [as shown in Figure 7(b)], while HA-*g*-PEGDMA in composite dispersed well at nano-scale [as shown in Figure 7(c)]. Detailed information of the HA particle is displayed in Figure 7(d), which indicated the morphologies of the precipitated nanoparticles like olive, with a length of about 100 nm and a width of about 30–50 nm.

Mechanical Properties

The mechanical properties of composites were evaluated by compressive tests. The compressive strength and modulus of PEGDMA, HA/PEGDMA, and HA-*g*-PEGMA/PEGDMA composites are shown in Table I. Compared with the pure poly(-PEGDMA), HA/PEGDMA and HA-*g*-PEGMA/PEGDMA composites exhibited higher compressive strength and modulus. The compressive strength and modulus of HA-*g*-PEGMA/PEGDMA composite increased with the increasing of content of nanoparticles until at 1 wt % of nanoparticles. The compressive strength and modulus of HA-*g*-PEGMA/PEGDMA composite were increased 14% and 9% compared with HA/PEGDMA, respectively. The improvement in compressive strength could be attributed to the enhancement of the interaction between nanoparticles and matrix and a better dispersion of filler in the matrix. This was due to the surface grafting of HAp nanoparticles. The PEGMA grafted onto the HA nanoparticles could prevent the particles from aggregating and thus improved the dispersibility of the nanoparticles in the poly(PEGDMA) matrix. Meanwhile, the double bond of PEGMA on the surface of HA could copolymerize with the matrix, enhanced interface combination of organic and inorganic phase. However, as persistence of content of HA-*g*-PEGMA increasing, the compressive strength and modulus of HA-*g*-PEGMA/PEGDMA composite decreased. The more content of nanoparticles could still result in serious aggregation. HA nanoparticle agglomerate could induce serious phase

Table I. Mechanical Properties of Composite Containing HA and HA-*g*-PEGMA

Content (wt %)	0	0.5		1		3		5	
	Pure PEGDMA	HA	HA-*g*-PEGMA	HA	HA-*g*-PEGMA	HA	HA-*g*-PEGMA	HA	HA-*g*-PEGMA
Compressive strength (MPa)	9.2 ± 0.3	9.4 ± 1.1	13.1 ± 0.9	13.1 ± 0.6	14.9 ± 1.1	13.0 ± 1.2	13.7 ± 1.2	12.4 ± 1.3	13.2 ± 1.6
Compressive modulus (MPa)	33.6 ± 0.8	32.3 ± 0.9	38.2 ± 1.5	37.6 ± 3.1	41.2 ± 0.2	40.8 ± 0.8	38.1 ± 3.5	41.0 ± 3.4	39.1 ± 4.5

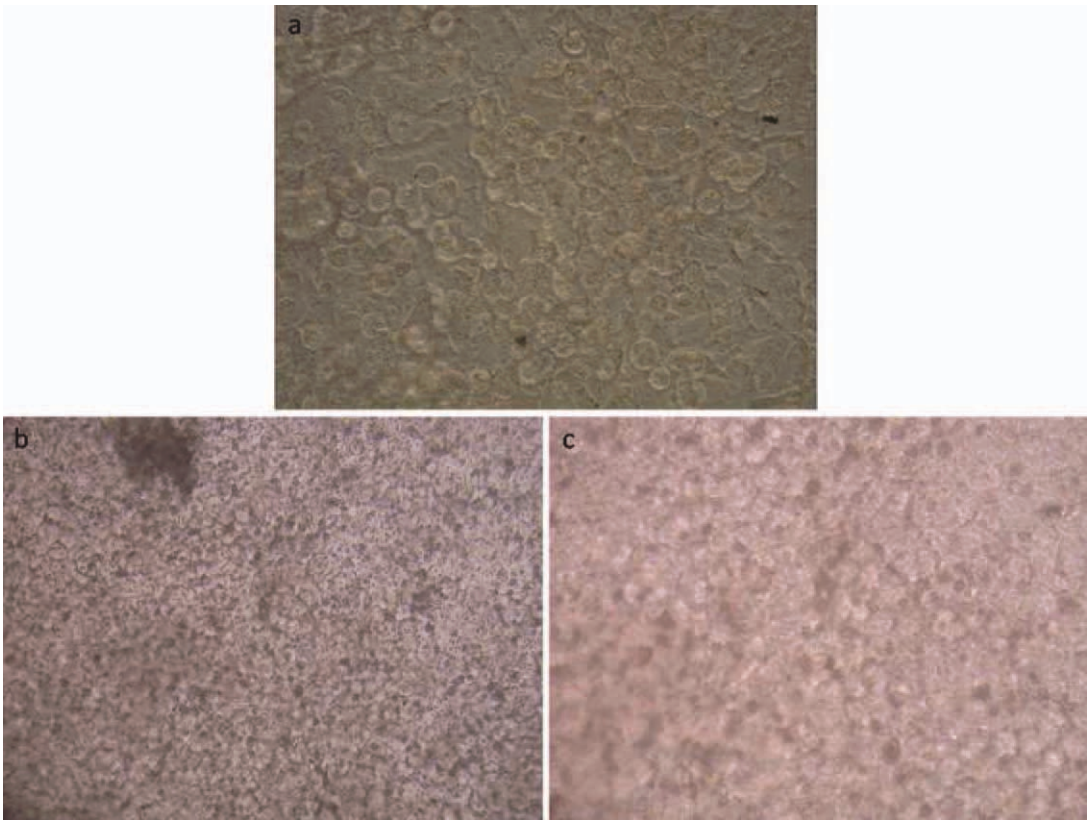

Figure 8. Cells observed by inverted phase contrast microscope. (a) composite with 0.0% HA, (b) composite with 1.0% HA, and (c) composite with 1.0% HA-*g*-PEGMA. [Color figure can be viewed in the online issue, which is available at wileyonlinelibrary.com.]

separation in the matrix. Then the composite network easily broke up. The literature[28] also reported that significant aggregation occurring in the HA particles within PLA matrix resulted in the deterioration of mechanical strength.

Cytocompatibility Test

Digital images of the hMSCs using an inverted phase contrast microscope after 3 days of culture (Figure 8) exhibited cell distribution over the visual field. There were lots of cells distributing on the surface of composite containing HA-*g*-PEGMA in Figure 8(c). There was no distinct difference between composites with HA and HA-*g*-PEGMA in Figure 8(b), while some cells are observed on the PEGMA without HA in Figure 8(a). HA-*g*-PEGMA nanoparticles could enhance hMSCs to grow, and would not bring in obvious cell damage.

CONCLUSIONS

In this study, to improve dispersibility of HA in the polymer matrix, the surface of HA particles was modified with PEGMA and the highest grafting ratio of PEGMA was about 6 wt %. The HA-*g*-PEGMA/PEGDMA composites showed improved mechanical properties compared to the corresponding HA/PEGDMA composites. The compressive strength and modulus of HA-*g*-PEGMA/PEGDMA composite were increased 14% and 9% compared with HA/PEGDMA, respectively. When content of HA-*g*-PEGMA continuously increased, the compressive strength and modulus would decrease. These results suggested that the surface of HA nanoparticles modified with PEGMA may be a superior way to improve the mechanical properties of the composites.

ACKNOWLEDGMENTS

The author would like to thank the National Natural Science Foundation of China (50803004), Beijing Natural Science Foundation (2112033 Study on the molecular design and properties of new photocurable antifouling coatings) and the Fundamental Research Funds for the Central Universities (ZZ1115) for its financial support.

REFERENCES

1. Kitsugi, T.; Yamamuro, T.; Nakamura T.; Kotani, S.; Kokubo, T. *Biomaterials* **1993,** *14*, 216.
2. Heise, U.; Osborn, J. F.; Duwe, F. *Int. Orthop.* **1990,** *14*, 329.
3. Van Blitterswijk, C. A.; Hesselling, S. C.; Grot, J. J.; Korerte, H. K.; de Groot, K. *J. Biomed. Mater. Res.* **1990,** *24*, 433.
4. Kurashina, K.; Kurita, H.; Takeuchi, H.; Hirano, M.; Klein, C.; de Groot, K. *Biomaterials* **1995,** *16*, 119.
5. Na, K.; Kim, S. W.; Sun, B. K.; Woo, D. G.; Yang, H. N.; Chung, H. M.; Park, K. H. *Biomaterials* **2007,** *28*, 2631.

6. Jao, Y.; Liu, Z.; Cui, F.; Zhou, C. *J. Bioact. Compat. Polym.* **2007,** *22*, 492.
7. Sionkowska, A.; Kozłowska, J. *Int. J. Biol. Macromol.* **2010,** *47*, 483.
8. Swetha, M.; Sahithi, K.; Moorthi, A.; Srinivasan, N.; Ramasamy, K.; Selvamurugan, N. *Int. J. Biol. Macromol.* **2010,** *47*, 1.
9. Han, J.; Zhou, Z.; Yin, R.; Yang, D.; Nie, J. *Int. J. Biol. Macromol.* **2009,** *46*, 199.
10. Madhumathi, K.; Shalumon, K. T.; Divya Rani, V. V.; Tamura, H.; Furuike, T.; Selvamurugan, N.; Nair, S. V.; Jayakumar, R. *Int. J. Biol. Macromol.* **2009,** *45*, 12.
11. Zhai, Y.; Cui, F. *J. Cryst. Growth* **2006,** *291*, 202.
12. Ruys, A. J.; Wei, M.; Sorrell, C. C.; Dickson, M. R.; Brandwood, A.; Milthorpe, B. K. *Biomaterials* **1995,** *16*, 409.
13. Lu, L.; Mikos, A. *MRS Bull.* **1996,** *21*, 28.
14. Hong, Z.; Qiu, X.; Sun, J.; Deng, M.; Chen, X.; Jing, X. *Polymer* **2004,** *45*, 6699.
15. Hong, Z.; Zhang, P.; He, C.; Qiu, X.; Liu, A.; Chen, L.; Chen, X.; Jing, X. *Biomaterials* **2005,** *26*, 6296.
16. Qiu, X.; Chen, L.; Hu, J.; Sun, J.; Hong, Z.; Liu, A.; Chen, X.; Jing, X. *J. Polym. Sci. Part A: Polym. Chem.* **2005,** *43*, 5177.
17. Liu, Q.; de Wijn, J. R.; de Groot, K.; van Blitterswijk, C. A. *Biomaterials* **1998,** *19*, 1067.
18. Liu, Q.; de Wijn, J. R.; van Blitterswijk, C. A. *J. Biomed. Mater. Res.* **1998,** *40*, 490.
19. Liu, Q.; de Wijn, J. R.; van Blitterswijk, C. A. *J. Biomed. Mater. Res.* **1998,** *40*, 257.
20. Pramanik, N.; Mohapatra, S.; Bhargava, P.; Pramanik, P. *Mater. Sci. Eng., C.* **2009,** *29*, 228.
21. Zhou, Z.; Ren, Y.; Yang, D.; Nie, J. *Biomed. Mater.* **2009, 4.**
22. Zhou, Z.; Yang, D.; Nie, J.; Ren, Y.; Cui, F. *J. Bioact. Compat. Polym.* **2009,** *24*, 405.
23. Lin-Gibson, S.; Bencherif, S.; Cooper, J. A.; Wetzel, S. J.; Antonucci, J. M.; Vogel, B. M.; Horkay, F.; Washburn, N. R. *Biomacromolecules* **2004,** *5*, 1280.
24. Yang, F.; Williams, C. G.; Wang, D. A.; Lee, H.; Manson, P. N.; Elisseeff, J. *Biomaterials* **2005,** *26*, 5991.
25. Murugan, R.; Ramakrishna, S. *Cryst. Growth Des.* **2005,** *5*, 111.
26. Shih, W. J.; Chen, Y. F.; Wang, M. C.; Hon, M. H. *J. Cryst. Growth* **2004,** *270*, 211.
27. Ashok, M.; Sundaran, N. M.; Kalkura, S. N. *Mater. Lett.* **2003,** *57*, 2066.
28. Li, J.; Lu, X. L.; Zheng, Y. F. *Appl. Surf. Sci.* **2008,** *255*, 494.